Arch Bridges
ARCH´04
P. Roca and E. Oñate (Eds)

DESIGN RECOMMENDATIONS FOR REINFORCED MASONRY ARCHES

Paulo B. Lourenço*, Késio Palácio* and Joaquim O. Barros*

* Universidade do Minho
Departamento de Engenharia Civil
Azurém, P-4800-058 Guimarães, Portugal
e-mail: pbl@civil.uminho.pt, web page: http://www.civil.uminho.pt/masonry

Key words: Elastic analysis, Limit analysis, Finite element analysis, Design

Abstract. *Very few publications address the analysis or design of reinforced masonry shells. In the paper, the usage of elastic and plastic approaches for the analysis and design of masonry arches is discussed, with respect to the application of a point load and a two-pinned arch. The results of a recent experimental program are also briefly reviewed and discussed in light of the results from numerical simulations using the finite element method. Finally, practical and conservative design recommendations are proposed.*

1 INTRODUCTION

Masonry vaults are one of the most common structural shapes present in the architectural heritage of almost all countries in the world. Still, renewed interest is arising recently with respect to this type of structures, for modern buildings and bridges. These structures are defined as structures in which the load bearing is clearly associated with the distribution of material in space.

Vaulted structures are usually considered as an ideal system of arches. Clearly, barrel vaults can be understood as a set of parallel arches, but also vaults of more complex shape can be generally outlined in a similar way, with a system of main arches that support secondary arches. It is noted that, in some cases, simplifications using ideal arched schemes lead to difficulties in justifying equilibrium, especially when the loads are not uniformly distributed[i]. Therefore, true 3D analysis and behavior might be necessary for more complex cases.

In this paper, a methodology for the analysis and design of reinforced arches is addressed. Since, in most cases, the analysis and design of vaults is possible using a subdivision into arches, the approach should be considered general. The standard techniques for simplified analysis and design criteria of arches include both elastic and plastic approaches. The proposed design criteria are compared with experimental values recently carried out in reinforced masonry vaults and numerical analysis using the finite element method, for validation purposes. The results are of interest both for the strengthening of existing masonry vaults and for the design of new reinforced masonry vaults.

2 DESIGN CRITERIA FOR VAULTS (PARABOLIC AND CATENARY ARCHES)

An engineering structure has to satisfy many functional requirements. Two of the most important requirements are that the structure is strong enough to resist the applied loading (including its own weight) without collapsing, and that the structure is stiff enough not to deflect unduly under such loading. To achieve this last functional requirement, the usual design procedures are based on the elastic behavior of the structure. On this basis, the strength of a structure is assessed from the observation or calculation of how close the structure is to yielding in any of its parts.

For materials and structures exhibiting plastic behavior, which normally includes arched structures, there is an alternative method of design called plastic method of design, or ultimate strength design. This method is based on the fact that structural elements cannot deflect indefinitely or collapse until a mechanism if formed. In the case of arches, beams or rigid frames, the requirement of a mechanism indicates that the full plastic moment Mp has developed at each of several critical sections. If it is assumed that the plastic moment acts at each such section, then the problem becomes statically determinate and the load corresponding to the collapse condition can be readily calculated.

Next, both elastic and plastic design approaches are addressed.

2.1 Elastic formulation

The adopted elastic formulation for curved members is based on the assumption that the cross-sectional dimensions of the member are small compared with the radius of curvature, so

that the stresses can be calculated by formulas applicable for straight members. Additionally, given the fact that elastic analysis is addressed, the effect of deformations on the bending moments may be neglected and the principle of superposition is applicable.

The evaluation of the maximum normal stresses σ in a cross-section of an arch, subjected to combined axial loading N and bending moment M, is given by

$$\sigma_{t,b} = \frac{N}{A} \pm \frac{M}{I} \cdot c_{t,b} \tag{1}$$

where A and I are respectively the area and inertia of the cross-section, c is the distance of the extreme fiber to the center of mass of the cross-section, and the subscripts t and b indicate the top and bottom fibers, respectively.

Figure 1 shows a two-pinned parabolic arch subjected to a single concentrated load P plus its own uniformly distributed weight q. The shape of the arch is assumed parabolic, due to the simplicity of the mathematical formulation, but the results can be adopted for catenary arches for design purposes, as the differences are only minor[ii]. The expression of the parabolic arch with a span $2L$ and a rise f is given by

$$y = \frac{f}{L^2} x^2 \tag{2}$$

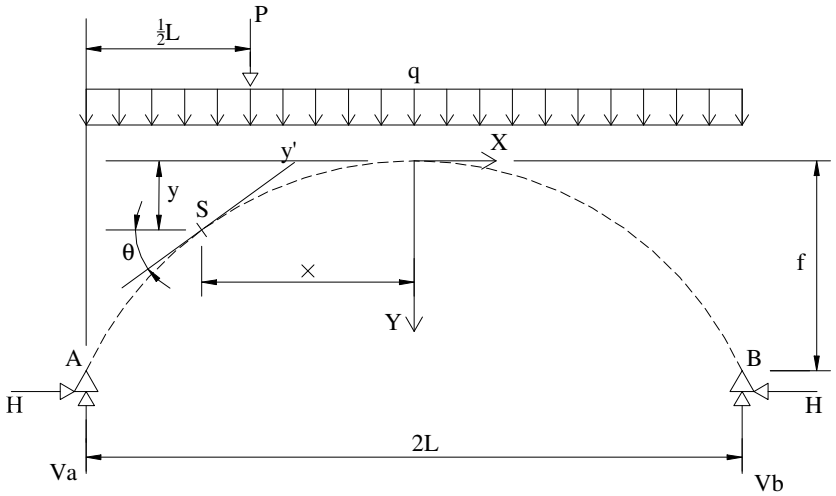

Figure 1: Two-pinned parabolic arch submitted to a single concentrated load P plus its own weight q

From the strength of materials[iii], the unknown hyperstatic reaction H may be determined by

$$H = \frac{\int_0^{2L} \frac{M_S \, y \cdot ds}{EI}}{\int_0^{2L} \frac{y^2 \cdot ds}{EI} + \int_0^{2L} \frac{ds}{EA}} \tag{3}$$

where M_S is the bending moment at section S, y is the vertical coordinate of the arch axis, A is the area of the cross-section and E is the Young's modulus of the material. In the present case, the value of H reads[ii]

$$H = \frac{\frac{61PL^2 f}{768I_o} + \frac{qL^3 f}{15I_o}}{\frac{8Lf^2}{15I_o} + \frac{L}{A_o}} \tag{4}$$

Once the horizontal reaction H is determined, it is possible to calculate the axial force N and the bending moment M at any section S of the arch, as

$$\begin{aligned} M_S(x,y)^1 &= V_A \cdot (x+L) - \frac{q\cdot(x+L)^2}{2} - H\cdot(f-y) && \text{for } -\mathrm{L} \le \mathrm{x} \le -\frac{\mathrm{L}}{2} \\ Ns(x,\theta)^1 &= q\cdot(x+L)\sin\theta - V_A\cdot\sin\theta - H\cdot\cos\theta \\ M_S(x,y)^2 &= V_A \cdot (x+L) - \frac{q\cdot(x+L)^2}{2} - \mathrm{P}\cdot\left[(\mathrm{x}+2) - \frac{\mathrm{L}}{2}\right] - H\cdot(f-y) && \text{for } -\frac{\mathrm{L}}{2} \le \mathrm{x} \le L \\ Ns(x,\theta)^2 &= q\cdot(x+L)\sin\theta - V_A\cdot\sin\theta - H\cdot\cos\theta \end{aligned} \tag{5}$$

Here, V_A is the vertical reaction at the left support, given by

$$V_A = \frac{3}{4}P + qL \tag{6}$$

From the internal forces N and M given by Eqs. (5), the calculation of the maximum stresses in the cross-section $\sigma_{b,t}$ is straightforward from Eq. (1) and dimensioning can be carried out using the standard ultimate limit state design procedures.

2.2 Plastic formulation

There are two methods of plastic design, namely the static and the kinematic method. Here, only the kinematic method is shown and the reader is referred to Palácio *et al.*[ii] for the elaboration of the static method, which can be particularly simple for this particular loading condition. The plastic formulation allows to determine the collapse load of a two-pinned parabolic arch subjected to a point load P. The self-weight of the arch will not be taken into account in order to simplify the analysis. It is stressed that this assumption does not affect the results significantly because the self-weight of the arch is usually much lower than the collapse load, for modern reinforced masonry arches.

To apply the kinematic approach and apply the principle of virtual work, it is necessary to define an admissible collapse mechanism. Failure of the arch occurs once two plastic hinges are formed. Therefore, it is possible to construct the collapse mechanism shown in Figure 2. The virtual work principle states that the external work δW_{ext} produced in any virtual deformation must be equal to the internal work δW_{int}, reading

$$P(L-a)\beta = Mp_1\cdot(1+\theta) + Mp_2\cdot(\alpha+\theta) \tag{7}$$

Here, the rotation angles α, β and θ of the rigid parts of the arch are defined in Figure 2 and

the vertical displacement of force P is given by $(L - a).\beta$. The plastic moments at the left and right hinges are respectively Mp_1 and Mp_2. To define the virtual deformed configuration, and for the sake of simplicity, the angle β was assumed equal to the unit value.

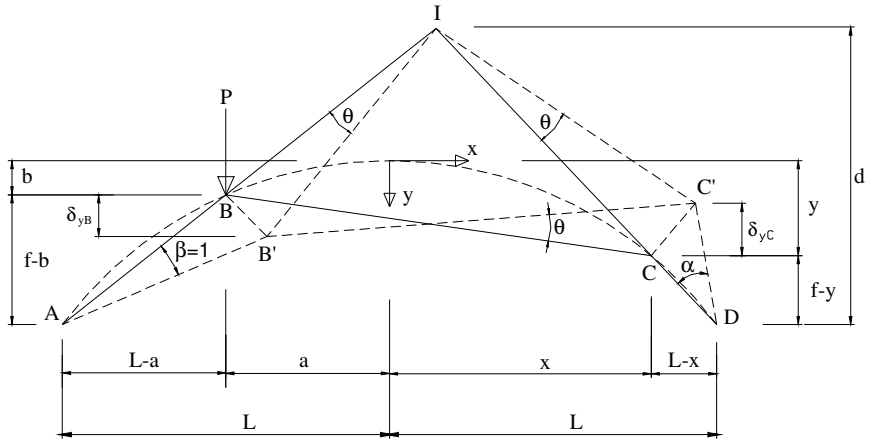

Figure 2: Collapse mechanism for the arch carrying a point load P

Angles α and θ can be expressed from[ii]

$$\alpha = \frac{d-(f-y)}{(f-y)} \cdot \frac{(f-b)}{d-(f-b)} \qquad \theta = \frac{f-b}{d-(f-b)} \tag{8}$$

With these values, Eq. (7) can be recast as

$$P = \frac{Mp_1}{L-a}\left(1 + \frac{f-b}{d-(f-b)}\right) + \frac{Mp_2}{L-a}\left(\frac{(f-b)}{d-(f-b)} \cdot \frac{d}{(f-y)}\right) \tag{9}$$

The quantity d can be expressed from[ii]

$$d = \frac{2 \cdot L}{\left(\frac{L-x}{f-y} + \frac{L-a}{f-b}\right)} \tag{10}$$

Finally, introducing this value of d in Eq. (9), replacing a by $L/2$, and introducing the parabolic shape, from which the values of b and y can be calculated, it is possible to obtain the value of the collapse load P_u

$$P_u = 48Mp_1 \cdot \frac{L+x}{(9L+18x) \cdot L} + 36Mp_2 \cdot \frac{L}{(9L+18x) \cdot (L-x)} \tag{11}$$

The location of the second plastic hinge is given by the unknown distance x, which can be obtained by taking a derivative of P with respect to x and setting it equal to zero. Thus,

$$\frac{dP}{dx} = 0 \Rightarrow \quad x = \frac{L}{8Mp_1} \cdot \left(8Mp_1 + 12Mp_2 - 12\sqrt{Mp_1 Mp_2 + (Mp_2)^2} \right) \tag{12}$$

Table 1 gives the values of x, obtained for selected values of Mp_1 and Mp_2. Once the location of the second hinge is known, Eq. (11) allows obtaining the value of the ultimate load P_u.

Mp_1	Mp_2	x	P_u
Mp	Mp	0.379L	15.70Mp/L
Mp	0.5Mp	0.451L	8.73Mp/L
Mp	0	L	3.56Mp/L

Table 1 : Values of the location x for the second plastic hinge and of the ultimate load P_u, for given values of Mp_1 and Mp_2

3 RESULTS FROM THE EXPERIMENTAL AND NUMERICAL PROGRAM

In order to validate the design procedures addresses in the previous chapter, experimental results[iv] in reinforced arches are briefly introduced, compared with elastic and plastic analysis, and also compared with the results of an advanced analysis tool using non-linear finite elements.

3.1 Test results

Sarralbo[iv] tested five reinforced masonry arches with catenary shape. Figure 3 illustrates the typical cross section of the arches, with a thickness h equal to 75 mm, a reinforcement depth d equal to 60 mm and a width b equal to 1.09 m. The span of the arches 2L is equal to 4.0 m, the rise f is equal to 1.0 m and the self-weight q is equal to 1.58 N/m.

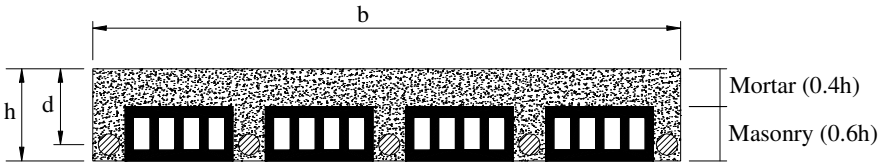

Figure 3: Cross-section of the arches

Table 2 presents the material properties and the collapse loads of the five vaults[iv]. Here ρ is the percentage of longitudinal reinforcement, f_y is the yield strength of the reinforcement (assumed equal to the Steel Class, as no tests have been carried out), $f_{c,\ cubes}$ is the compressive strength of the mortar measured in cubes, f_{cm} is the calculated actual compressive strength of the mortar and f_{tm} is the tensile strength of the mortar.

The calculated compressive strength of mortar f_{cm} is equal to 0.8 $f_{c,\ cubes}$, because the experimental values have been obtained in mortar cubic specimens according to EN 1015-11. In the case of vault 1 / 2, the tests to determine the tensile strength of the mortar f_{tm}, were not carried out. Therefore, the tensile strength has been estimated from MC90[v]. In the case of vault 3, a very high value was reported[iv] and the value shown is extrapolated from vault 4.

Vault	Reinforcement			Mortar				P_u (kN)
	No. of bars	ρ (%)	f_y (N/mm^2)	Strength (N/mm^2)	$f_{c,\,cubes}$ (N/mm^2)	f_{cm}* (N/mm^2)	f_{tm} (N/mm^2)	
1 / 2	5 ϕ 8	0.31	500	Low	13.0 / 21.0	16.8	1.29*	21.0
3	5 ϕ 8	0.31	500	High	56.3	45.0	2.20**	26.0
4	5 ϕ 6	0.17	400	High	53.5	42.8	2.00	15.2
5	5 ϕ 6	0.17	400	Low	38.6	22.6	1.70	14.2

Table 2 : Material and geometry properties and collapse loads for the vaults (* calculated; ** estimated)

With respect to the experimental values obtained for the distance x, which gives the location of formation of the second plastic hinge, no precise information exists even if it is reported that, for all the tested vaults, the second hinge is in a region symmetrical to the position of the application of load P[iv].

3.2 Elastic and plastic analysis

Ultimate limit state design of reinforced masonry shells requires detailing of reinforcement to cover all zones where tensile stresses may appear. This calls for upper and lower reinforcement in the vaults for the combination of distributed loading and a point load. As there is no upper (extrados) reinforcement in the tested vaults, elastic analysis can only be used up to cracking of the upper layer of the vault.

Table 3 presents the results of the internal forces N and M at sections S_1 (left plastic hinge) and S_2 (right plastic hinge) and the corresponding stresses at the extreme fibers. The results were obtained using Eq. (5)[ii]. The maximum tensile strength is reached at a position x, which indicates the most likely location of the "plastic" hinge for limit analysis. It is noted that the maximum tensile stresses occur in the cross-section under the load application (left hinge). Nevertheless, as this region includes bottom reinforcement, the critical section is, indeed, the right plastic hinge.

Vault	Left plastic hinge		Right plastic hinge	
	N_1 (kN)	M_1 (kN.m)	N_2 (kN)	M_2 (kN.m)
1 / 2	-9.26	2.03	-7.66	-1.34
3	-13.57	3.54	-10.86	-2.33
4	-12.79	3.27	-10.27	-2.15
5	-11.38	2.78	-9.23	-1.82

Table 3 : Numerical results for elastic analysis

Design of the masonry vaults, reinforced only at the bottom (intrados), is better carried out using plastic analysis. According to the formulas of plastic design presented to determinate the collapse load P_u, Eq. (11), it is necessary to know the values of the plastic moments at the left and right hinges, respectively Mp_1 and Mp_2. However, since the cross section of the arch is subjected to combined bending and compression, it is necessary to consider the interaction

of the bending moment M and the normal force N. This N-M interaction diagram can then be used for taking into account the internal forces acting in the cross-section. Thus, the N-M interaction diagram for each vault must be constructed and, because the axial loading depends on the point load P_u at ultimate stage, an iterative process should be adopted for the calculation of the plastic limit load[ii].

Table 4 shows the results for the ultimate loads obtained with elastic and plastic (limit) analysis. For the right hinge of plastic analysis, tensile strength has been taken into account.

Vault	P_u Testing (kN)	Elastic analysis			Plastic analysis		
		x (mm)	P^e_u (kN)	$\frac{P^e_u}{P_u}$	x (mm)	P^p_u (kN)	$\frac{P^p_u}{P_u}$
1 / 2	21.0	828	6.68	0.32	1147	17.96	0.86
3	26.0	816	11.65	0.45	1029	21.00	0.81
4	15.2	800	10.75	0.71	876	11.97	0.79
5	14.2	812	9.13	0.64	910	11.27	0.79

Table 4 : Comparisons between calculated and testing P_u

As it is normal in concrete structures, cracking occurs before collapse (between 30% and 70% of the maximum load). After cracking significant load redistributions occur, as mortar possesses a quasi-brittle behavior. The amount of bottom reinforcement necessary at the cracking stage, and the existing reinforcement can be compared[ii]. The ratio between loads is rather different from the ratio between reinforcements, meaning that elastic design cannot be used unless top and bottom reinforcement are considered. However, elastic analysis can be of interest as a tool to define the position of the second (right) hinge.

Clearly, in terms of ultimate load, the results from plastic analysis are much better than those of elastic analysis. Nevertheless, the plastic analysis results still lay around 15% to 20% below the experimental load, even if the cracking moment at the right hinge Mp_2 is assumed as fully plastic. It is believed that the main reason for the differences found are due to the lack of information on the constitutive behavior of the adopted steel. It is noted that the relation between the calculated ultimate load and the observed failure load does not vary significantly. Another interesting aspect is that the iterative process adopted[ii] allows for (moderate) variation of the location of the plastic hinge x. This procedure is also questionable because, once the crack occurs in the top surface, the location of the "hinge" is fixed.

3.3 Finite Element Method analysis

Eight-noded plane stress elements were in the finite element analysis. The adopted non-linear material model is based on a smeared crack model (fixed cracked model), specified as a combination of tension cut-off (two orthogonal cracks), tension softening and shear retention, combined with a plasticity-based criterion in compression. The reader referred to Rots[vi] for further reading. The reinforcement was modeled with embedded reinforcement superimposed elements, with a Von Mises yield criterion. Full details on the material properties are given in Palácio *et al*[vii].

The numerical results are in reasonable agreement with the experimental results, in terms of collapse load and arch behavior. A typical four-hinged collapse mechanism was found in the analyses, as adopted above for limit analysis. The ductile response of the shell is due to yielding of reinforcement at the left hinge, previous to mortar crushing. As shown in Figure 4, the initial stiffness obtained in the numerical analysis is rather high, followed by a sharp drop of strength, associated with cracking of the right hinge. This is confirmed by Sarralbo[iv], who refers cracking of the right hinge as the first sign of inelastic behavior. It is noted that the first peak and high stiffness do not occur in the experimental tests, which is probably due to a very low tensile strength of the upper layer, related to the difficulties in placing the mortar.

A sensitivity analysis[vii] indicated that the tensile strength and yield strength of the reinforcement affect the results. Limit analysis reproduces well the numerical results, with the exception of series 4, in which a sharp drop of load is obtained after the first crack. Provisions to ensure a ductile post-peak behavior are therefore required for design.

4 DESIGN RECOMMENDATIONS

In the previous chapter, the tensile strength was considered for the sake of assessment of plastic analysis. This hypothesis is questionable from the theoretical point of view but also from a practical point of view, as it constitutes a violation with respect to codes. In fact, the tensile strength of cement-based materials should be considered equal to zero for the verification of the ultimate limit states.

In order to eliminate the drawback of the previous approach to solve engineering applications, one possibility is to use the location of the right hinge according to the elastic analysis. In the absence of upper reinforcement, this is the most likely location of the right hinge. Also, the influence of the axial force is usually negligible and can be ignored for practical purposes. With these assumption, it is possible to adopt $Mp_2 = 0$ (the collapse mechanism is perfectly defined) and an iterative procedure for solution is no longer required. Eq. (11) is directly applicable as the location of the right hinge x is no longer resulting from a minimization process. This approach leads to results between 50% and 75% of the experimental failure loads[ii], which are conservative values adequate for practical applications.

5 CONCLUSIONS

Elastic analysis is inadequate to analyze arches, unless upper and lower reinforcement are provided. In the case of placing both upper and lower reinforcement, the usage of elastic analysis does not allow load redistributions. An iterative procedure to calculate the ultimate load using plastic analysis is required. As tension appears in the extrados and intrados of an arch subjected to point loads, a minimum ratio of reinforcement is required in both sides.

11 ACKNOWLEDGEMENTS

This work was sponsored partly by the Portuguese Science and Technology Foundation (FCT), contract POCTI-ECM-38071-2001, “Strengthening of masonry arches with composite materials” and partly by the European Commission, contract GROW-1999-70420, “Industrialized Solutions for Construction of Masonry Shell Roofs”.

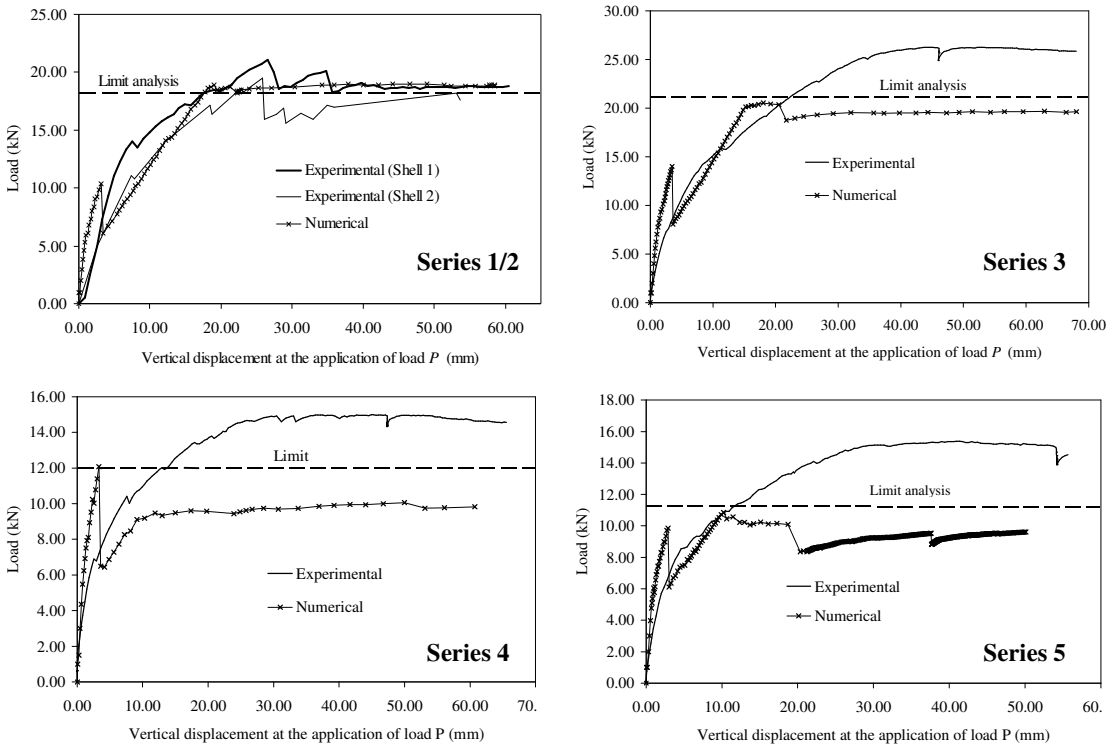

Figure 4: Experimental vs. numerical load-displacement diagrams, at quarter span

REFERENCES

[i] E. Giuriani, A. Gubana and A. Arenghi, "Structural rehabilitation of masonry vaults", in: Proceedings from the UNESCO-ICOMOS Millennium Congress, Paris (2001).

[ii] K. Palácio, P.B. Lourenço and J.O. Barros, *Task 1.3 - Contribution to design criteria for industrialized masonry vaults*, University of Minho, Report 03-DEC/E-10 (2003).

[iii] F. Rodriguez and A. Azcunaga, *Strength of materials (in Spanish)*, ETSII, Madrid, p. 51-71 (1980)

[iv] V. Sarralbo, *Contribution to the viability of laminar reinforced masonry roofs using semi-prefabricated solutions. Proposal for short span cylindrical shells (in Spanish)*, PhD Thesis, Universitat Politècnica de Catalunya, Barcelona (2002).

[v] CEB, *CEB-FIP Model Code 1990*, Bulletin d'Information nº 213/214, Thomas Telford, London (1993).

[vi] Rots, J.G., *Computational modeling of concrete fracture*, PhD thesis, Delft University of Technology, Delft (1988).

[vii] K. Palácio, P.B. Lourenço and J.O. Barros, Numerical modeling of single shell roofs, University of Minho, Report 03-DEC/E-21 (2003)